On the Design of Single-Point Cable-Linked Moorings for Ocean Observatories

Seon M. Han and Mark A. Grosenbaugh

***Abstract*—The goal of this paper is to provide design criteria for moorings proposed for long-term ocean observatories that use electro-optical-mechanical (EOM) cables and to identify the parameters that affect their dynamics. The EOM cables are much stiffer than traditional mooring lines, and therefore, the moorings may experience higher loads under most environmental conditions if not designed properly. Two designs that provide geometric compliance yet keep all the cable in the water column are considered. One of the designs uses a single subsurface float (SSF) with an "S-tether" positioned above it. The other design uses distributed buoyancy to create an S-tether in the lower half of the mooring line. Both designs use an elastomeric snubber hose attached inline just below the buoy. The maximum tensions in the hose and at the anchor and Raoof's contact stress-slip parameter at critical locations are used to evaluate the designs. The present results show that the most important design parameter in terms of the maximum tensions is the length of the mooring, the most important parameters in terms of the bending fatigue damage is the length of the buoyant section and the distribution of cable floats, and the most important design parameter in terms of the dynamic motion of the cable is the length of the snubber hose. In the design with an SSF, it is shown that there exists an optimum S-tether length that minimizes the maximum tensions for a given SSF depth. The general rule of thumb that the S-tether be about twice the depth of the SSF breaks down when the SSF is placed near the surface. In general, the design with an SSF should be used if a small watch circle and small tension in the snubber are required. The design without an SSF is preferred if small overall tension along the length of the mooring is required, if the bending fatigue failure is of concern, and if a longer smooth section of the cable below the surface buoy for use with a profiler is required. In both designs, the snubber length should be at least 30 m so that the dynamic motion is kept reasonably small.**

***Index Terms*—Electro-optical-mechanical (EOM) cable, inverse catenary, moored ocean observatories, oceanographic moorings, S-tether.**

I. Introduction

OVER the next decade, much of oceanographic research will be conducted using long-term measurements from ocean observatories [1]–[4]. The observatories will consist of suites of instruments mounted near the ocean surface, in the water column, and on the seafloor. A major component of the observatory system will be moored surface buoys, which will provide high-bandwidth "real-time" two-way communication links via satellite to remote sites around the world's oceans. The proposed mooring systems include trimoored spar buoys that will be deployed for up to ten years and more portable single-point moorings that will be deployed for three to five years. This paper concentrates on the single-point moorings by providing a quantitative framework for their design.

The single-point moorings that are proposed for ocean observatories will use an electro-optical-mechanical (EOM) cable as the mooring line. This is used to send power from the buoy to the seafloor and transmit data from the instruments to the buoy. The material used in EOM cables is typically much stiffer than that used in traditional oceanographic mooring lines, which consist of long lengths of nylon for elastic compliancy. Because of higher elastic stiffness, a mooring made from an EOM cable will experience higher loads under most current and wave conditions. In addition, failures in the communication and power paths can occur, regardless of the integrity of the cable itself, due to a mismatch between the stress–strain characteristics of the EOM cable's strength member and the internal bundles of copper conductors and optical fibers [5].

In this paper, it has been chosen to analyze two single-point mooring designs that are being considered for observatory mooring systems [1] with the idea of optimizing parameters that affect the failure of the mooring line and the internal conductors and fibers. These single-point moorings use solar panels on the buoy for power production and can transmit to shore up to 5 Mb of data per day. They are relatively cheap to build (compared with the trimoored spar buoy system) and easy to deploy requiring only a single ship. The first design uses an "S-tether" positioned above subsurface float (SSF) [Fig. 1(a)]. The S-tether is an EOM cable (as is the mooring line below the SSF) that is made positively buoyant (by attaching flotation) over roughly half of the cable and made negatively buoyant (by using steel-armored cable or attaching weights) over the other half of the cable. In light to moderate currents, the tether above the SSF forms an S-shape. The second design has a more traditional inverse catenary shape (without an SSF), which is formed by attaching flotation over the lower part of the mooring. The idea behind the S-tether and inverse catenary shapes is to increase the scope while preventing excess mooring line from chafing on the sea bottom in low currents. In both cases, an elastomeric hose is attached in-line below the buoy to increase elastic compliance in waves [5].

An early mention of an S-shaped mooring line with an SSF for oceanographic use appears in the work of Evans and Adamchack [6], where such a line is referred to as a slack mooring. A similar terminology was used by Berteaux [7] for an inverse

Manuscript received October 17, 2003; accepted December 13, 2004. This work was supported by the U.S. Office of Naval Research (Ocean Engineering and Marine Systems) under Grant N00014-92-J-1269 and the Deep Ocean Exploration Institute of Woods Hole Oceanographic Institution. The work of S. M. Han was supported in part by the Woods Hole Oceanographic Institution Postdoctoral Fellowship. **Associate Editor: H. Maeda**.

S. M. Han is with the Department of Mechanical Engineering, Texas Tech University, Lubbock, TX 79409 USA (e-mail: seon.han@coe.ttu.edu).

M. A. Grosenbaugh is with Woods Hole Oceanographic Institution, Woods Hole, MA 02543 USA (e-mail: mgrosenbaugh@whoi.edu).

Digital Object Identifier 10.1109/JOE.2005.850917

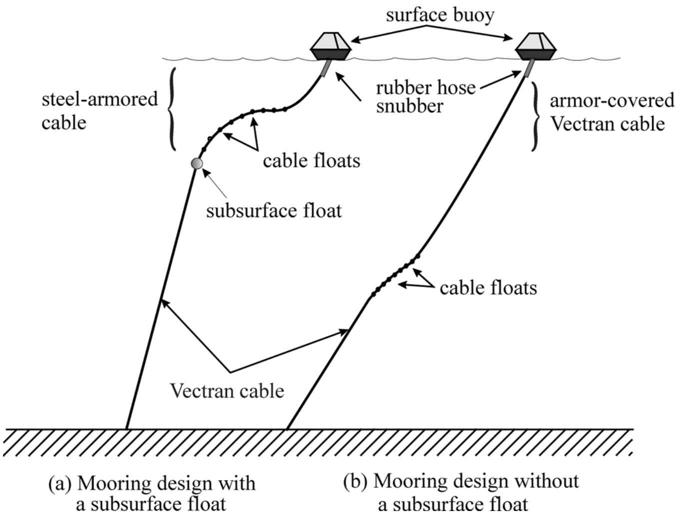

Fig. 1. Schematics of two mooring systems proposed for ocean observatories.

catenary mooring (without an SSF) made from a combination of polypropylene and nylon ropes. The National Data Buoy Center (NDBC) has been using inverse catenary moorings for coastal observation moorings in water depth greater than 600 m [8]. The oil industry has adopted S-shapes in the design of flexible risers since 1978, when flexible risers were first specified and installed in the Enchova field, offshore Brazil, as part of a floating production system [9]. Some of the basic configurations currently in service are the lazy-S, lazy-wave, steep-S, and steep-wave. The guidelines for installing such flexible pipes can be found in the publication RP-17B of the American Petroleum Institute [10]. Seyed and Patel [11] conducted a parametric study on these four types of flexible riser configurations for offshore petroleum applications.

The design issues for single-point oceanographic moorings that use EOM cables differ from those found in offshore oil industry because of the small-diameter cables that are used and the fact that the EOM cables must serve as the strength element in accommodating both dynamic motion and static offset. So far, the design of S-shaped tethers for oceanographic moorings has involved guess work without really knowing what effect changing the different parameters has on the cable motions and mooring forces. For example, it is not clear how deep the SSF should be placed and how buoyant it should be. Or, what is the effect of not using an SSF at all. Additional questions regarding the S-tethers and inverse catenary shapes are as follows: How long should the mooring line be? What percentage of its length should be positively buoyant and what percentage should be negatively buoyant? How buoyant should the buoyant section be? How heavy should the weighted section be?

The purpose of this work is to provide answers to these questions by evaluating the motion, tension, and fatigue damage of EOM mooring cables of single-point ocean observatory moorings subjected to current, wind, and random waves. Fatigue damage is estimated using by Raoof's contact stress-slip parameter defined in the subsequent section. Raoof's results are applicable in the strictest sense to steel-armored cables, which are used in the upper section of the mooring with an SSF. For synthetic mooring cables, which are used in the inverse catenary design and in the lower section of the mooring with an SSF, the assumption that the results can be applied in a relative sense is made (comparing two different mooring designs), though more research on the fatigue of synthetic cables is needed.

II. Raoof's Results

For a uniform rod, the bending moment is proportional to the curvature. The maximum stress due to bending occurs in the outer fiber, furthest away from the neutral axis. In the case of a strand of wire rope (with a king wire at the center and the layers of wires wound around it), it is tempting to calculate the stresses in the individual wires by assuming that they are uniform rods with negligible friction between them. However, experimental data show that when a strand fails in bending, it almost always fails near the neutral axis of the cable [10], where the relative motion between the outer two layers is the largest. This reveals that the friction must play an important role in the bending fatigue of cables. In fact, failure is due to the stress caused by the interlayer fretting or sawing actions between the two layers. The fatigue damage caused by interlayer fretting depends on the relative motion between the two layers. The relative motion increases with increasing amplitude of alternating curvature. For a cable under constant tension and alternating curvature (from κ to $-\kappa$), Raoof and Hobbs [12] and Raoof [13]–[15] showed experimentally that a single $S-N$ curve could be drawn in terms of the "contact stress-slip parameter" for cables with various dimensions and construction methods. The contact stress-slip parameter depends on the construction method (lay angles, wire radii, helix angle, etc.), mean axial strain, and the alternating curvature. The contact stress-slip parameter, which will be denoted as Λ, is given by

$$\Lambda = \frac{\sigma_x U_x}{x} \tag{1}$$

where σ_x is the normal stress that largely depends on the mean strain of the cable, x is the contact patch spacing, and U_x is the increase of x during bending of the cable and largely depends on the curvature. Raoof and Hobbs [12] and Raoof [13]–[15] describe how to obtain these quantities for a given strand of steel cable.

Raoof's result is for cables that are subjected to constant tension and alternating constant amplitude curvature with zero mean. In this case, the mean tension is slowly varying and can be assumed constant. However, the curvature varies randomly with time about the nonzero mean curvature. No research has been done to assess the effect that nonzero mean curvature or random loading has on the bending fatigue of cables. However, the goal of this paper is not to predict the fatigue life of a given mooring system but to compare various designs. For example, if both the mean and the standard deviation of Λ of a certain design are smaller than those of another design, it can be concluded that it is a better design. In this paper, the mean and the standard deviation of the contact stress-slip parameter will be plotted at critical locations along the mooring cable.

III. Design Analysis

Responses of the moored buoy systems are obtained using Woods Hole Oceanographic Institution (WHOI) cable, a gen-

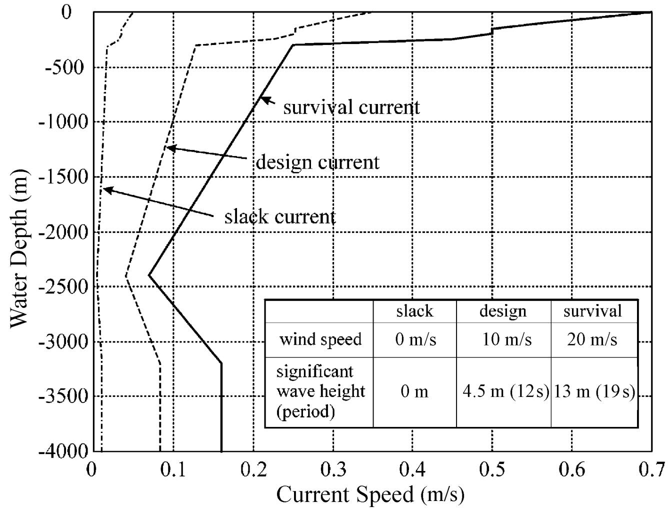

Fig. 2. Current profile.

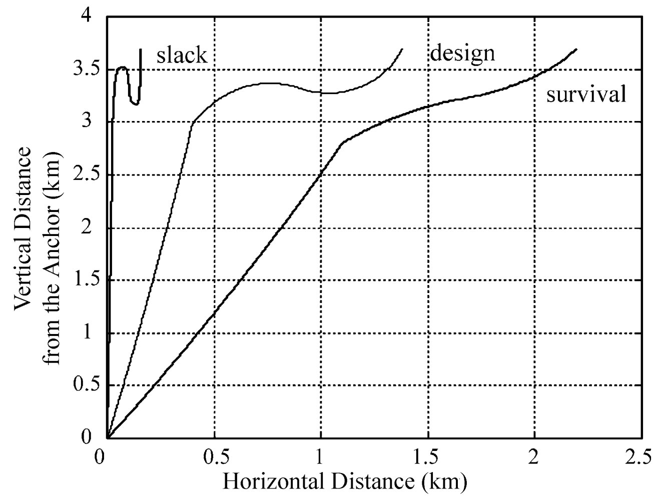

Fig. 3. Static configurations of the mooring with a SSF under the slack, design, and survival currents.

eral-purpose numerical code that was developed at WHOI for calculating the static and dynamic response of moored and towed oceanographic systems [16]. The finite-difference time-domain (FDTD) simulation is built around a mathematical model of cable dynamics. The cable model is fully three-dimensional (3-D) and includes the effects of torsion, bending, and geometric and material nonlinearities. The code has undergone extensive verification on a number of different cable systems [17], [18].

It is assumed that the vertical displacement of the surface buoy follows the wave elevation, which is described by a modified Pierson–Moskowitz spectrum. This assumption is valid because the proposed buoy shapes all have large water-plane areas relative to their virtual mass. The current speed profile, wind speeds, and significant waveheights that are used in the analysis are shown in Fig. 2. Values are given for slack water conditions, design conditions (the conditions that are expected to be exceeded 10% of the time), and survival conditions (25-year return storm). These values correspond to conditions that would be found along the Northern California coast, where seafloor observatory sites have been proposed. The design drivers are the maximum tension in the snubber hose, the maximum tension at the anchor, and the maximum bending fatigue along the mooring line. In each case, the maximum is defined as the mean value plus four times the standard deviation.

A. *Mooring With a Subsurface Float*

The properties of the baseline design with SSF are given in the Appendix. The baseline design consists of a surface buoy followed by a 30-m elastic snubber hose, a 700-m steel-armored EOM cable, a 700-m steel-armored EOM cable with thirty-six 272-N (61 lb) cable floats (they clamp directly onto the cable without releasing bending moments) placed at 20-m intervals, a 5-m chain potted in polyurethane and covered with tygon tubing (used at cable terminations), an SSF with a buoyancy of 10 200 N (2300 lb), a 5-m potted chain, a 2990-m Vectran EOM cable, a 5-m potted chain, and a 2730-kg (6000 lb) anchor. The wet weights of the buoyant section (with attached flotation) and the weighted section are about ±6.80 N/m, respectively. The baseline water depth of 3700 m was chosen to correspond with the Northern California location identified by Chaffey *et al.* [3] as a possible deployment site for their system. The scope of the baseline system is 1.2.

Fig. 3 shows the static configurations of the baseline mooring under the slack, design, and survival current and wind conditions. The S-shape is visible in the results for slack and design conditions. In survival conditions, the upper tether is nearly straight. In the survival case, the surface buoy has a horizontal offset of 2200 m. The theoretical maximum horizontal offset corresponds to when the mooring forms a straight line from the anchor to the surface buoy. Assuming that the cable is inextensible, the maximum horizontal offset is given by

$$x_{\mathrm{SB,max}} = \sqrt{s^2 - 1} \times D \tag{2}$$

where $x_{\mathrm{SB,max}}$ is the maximum possible horizontal offset of the surface buoy, s is the scope of the mooring, and D is the water depth. For the mooring considered in this case, the maximum horizontal offset is 2450 m.

Fig. 4(a) and (b) shows the mean tension T_{mean} and the standard deviation of the tension T_{std} along the cable from the anchor to the surface float in design and survival conditions due to the combined effects of wind, current, and waves. The highest values of T_{mean} for design and survival conditions occur just below the SSF. The highest dynamic tensions for design and survival conditions occur in the snubber. Most of the dynamic tension at the surface is transmitted to the anchor. This is true for both the design and survival conditions. Specifically, T_{std} at the anchor is about 81% of T_{std} in the snubber for the design case and about 95% of T_{std} in the snubber for the survival case. Fig. 4(c) shows the root mean square (rms) speed V_{rms} along the cable. The rms speed at 500 m below the SSF is only about 27% of the rms speed at the snubber for the design case and 31% of the rms speed at the snubber for the survival case. Table I shows the maximum tensions in the snubber and the anchor under the design and survival conditions. The working load of the snubber is about 17 800 N (4000 lb). The maximum tension at the anchor

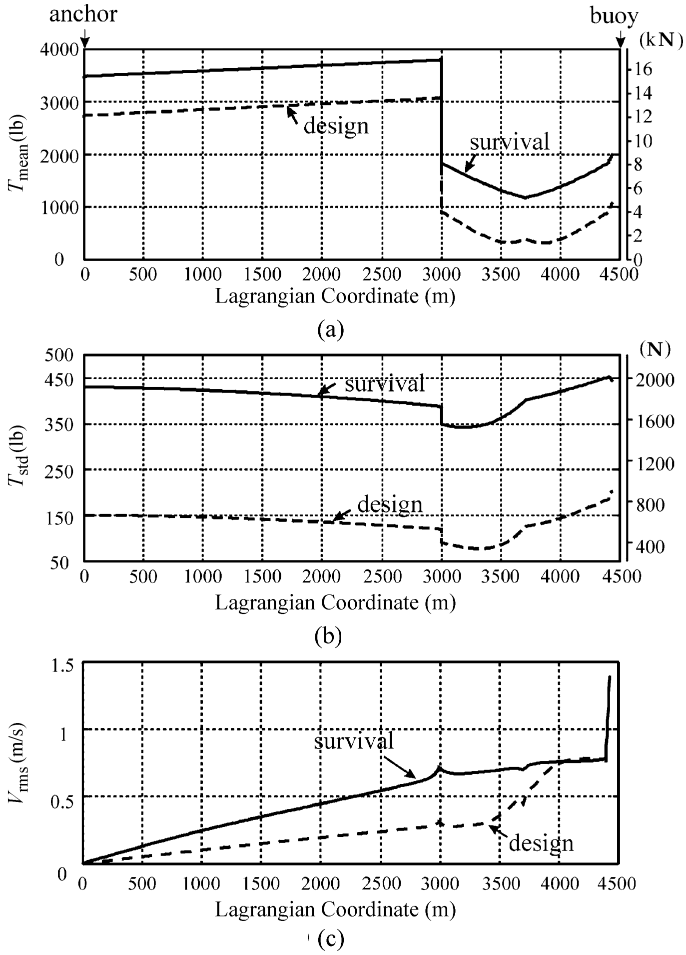

Fig. 4. Mean and standard deviation of the tension and rms speed under the design and survival conditions.

TABLE I
MAXIMUM TENSIONS OF BASELINE DESIGN WITH AN SSF

$T_{\max} = T_{\text{mean}} + 4T_{\text{std}}$	Snubber (N)	Anchor (N)
Design condition	8420	14 700
Survival condition	16 700	23 000

under survival conditions is about 1.6 times those under the design condition.

Fig. 5 shows mean and the standard deviation of the contact stress parameters Λ_{mean} and Λ_{std}, respectively, along the cable between the outermost and the second outermost layers of the cable. It has been assumed that both the steel-armored EOM cable (above the SSF) and the Vectran EOM cable (below the SSF) are constructed with a center core wrapped with five layers of strands (Table VII) similar to regular steel-cable construction. In reality, the inner layers of EOM cables are replaced with copper conductor and optical fiber bundles with two or three layers of strength members (steel strands or Vectran fibers) wrapped around the outside. For the calculations, it is assumed that the potted chain sections just above and below the SSF are constructed in such a way that the moments are not released. This is consistent with observations of actual cable bending failures in this type of mooring. Due to these assumptions, the only

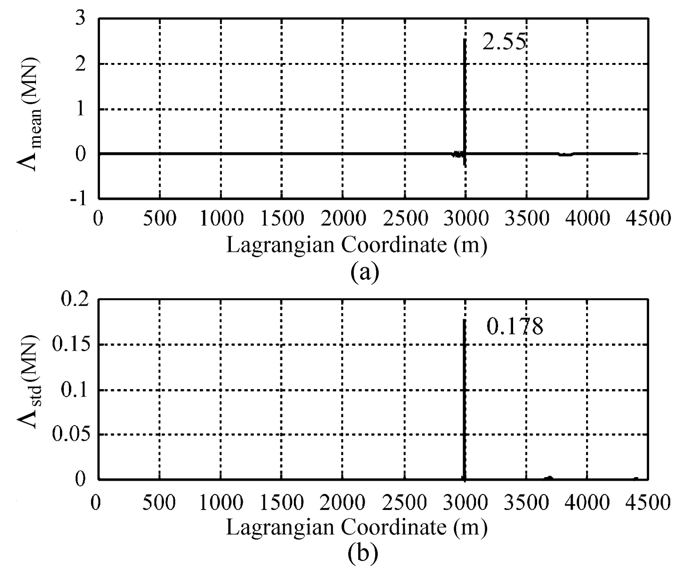

Fig. 5. Mean and standard deviation of the contact stress-slip parameter.

location of high Λ_{mean} and Λ_{std} is just above the SSF. For the remainder of this section, Λ_{mean} and Λ_{std} will be monitored only at this location. It should be noted that the contact stress-slip parameter takes the tension as well as bending curvature into account. Since the tension of the present mooring does not vary significantly along the cable, the plot of the contact stress-slip parameter in Fig. 5 is quite similar to that of the dynamic curvature.

1) Configuration Under the Slack Condition: Before performing a parametric analysis using wave forcing, the basic S-tether design that is required so that under slack conditions, the top loop of the S-tether does not interfere with surface activities (e.g., ships) or the bottom loop does not become tangled with the SSF is examined. If the horizontal distance between the SSF and the surface buoy is small, then

$$l = \frac{L - d}{2} \tag{3}$$

and

$$d_1 + d_2 = d - l \tag{4}$$

where l is the distance between the top and bottom of the S-tether, L is the total length of the S-tether, d is the SSF depth, d_1 is the clearance between the surface and the top of the S-tether, and d_2 is the clearance between the SSF and the bottom of the S-tether, as shown in Fig. 6. In addition, the total length of the S-tether L should not exceed three times the SSF depth or

$$L < 3d. \tag{5}$$

Intuitively, the depth of the S-tether under slack conditions depends on the length of the buoyant section, the buoyancy of the buoyant section, and the total length of the S-tether. Fig. 7 shows, for the baseline design, the locations of the top of the

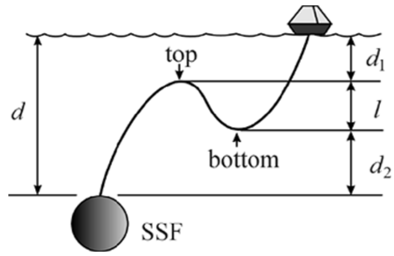

Fig. 6. S-tether configuration under the slack condition.

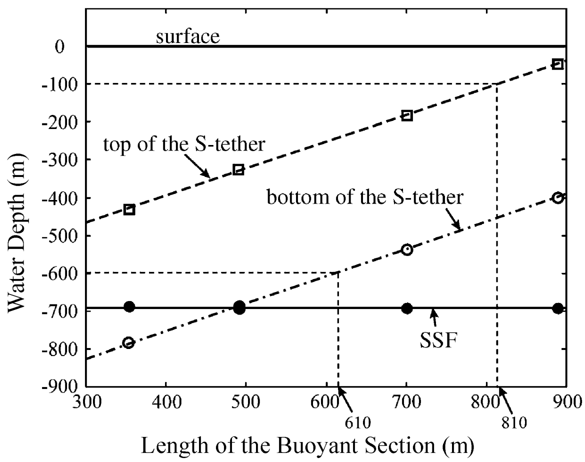

Fig. 7. Location of the S-tether when buoyant section length is varied under the slack condition.

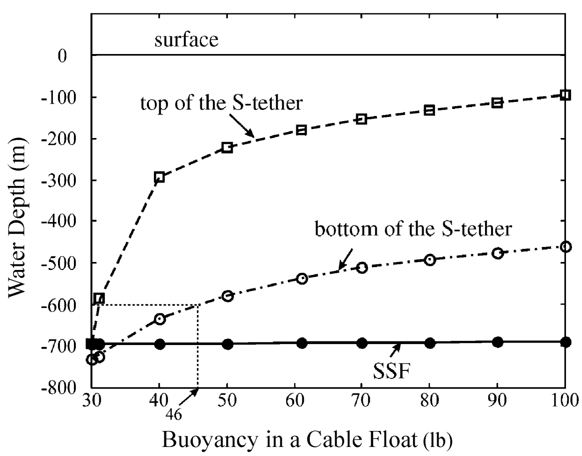

Fig. 8. Location of the S-tether when cable float buoyancy is varied under the slack condition.

S-tether, bottom of the S-tether, and the SSF under slack conditions when the length of buoyant section is varied while keeping the total length of the S-tether and the number of floats (i.e., the total buoyancy) constant. Extrapolating Fig. 7 linearly, it is found that the S-tether may come out of the water if the length of the buoyant section is longer than 960 m. If, for example, the top of the S-tether is required to be at least 100 m below the surface and the bottom of the S-tether to be at least 100 m above the SSF (d_1 >100 m and d_2 >100 m), then the length of the buoyant section must be between 610 and 810 m or 44–58% of the S-tether.

Fig. 8 shows the depth range of the S-tether under slack condition when the buoyancy of the cable floats is varied from 114

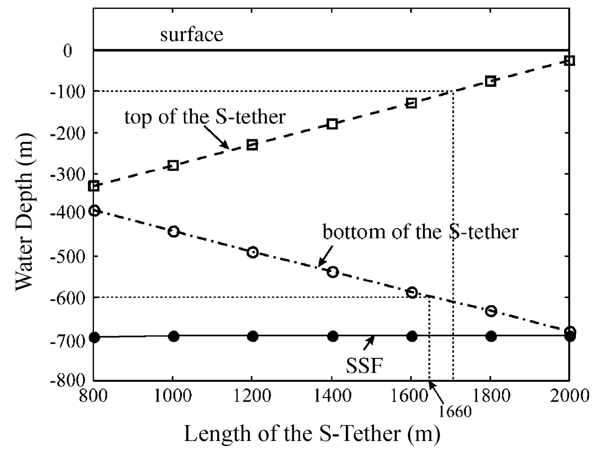

Fig. 9. Location of the S-tether when S-tether length is varied under the slack condition.

to 446 N (from 30.0 to 100 lb) while the length of the S-tether is kept constant at 1400 m and the length of the buoyant section remains at 700 m. Equivalently, the wet weight per unit length of the buoyant section is varied from -0.0657 to -16.09 N/m, where negative wet weight means that it is buoyant. When the buoyancy of each cable float is 113.6 N (30 lb), the buoyant section is nearly neutrally buoyant. Again, as an example, if it is required that the clearances are at least 100 m, the buoyancy of each cable float must be between 205 and 446 N (46.0 and 100 lb). The simple rule for the distance between the top and the bottom of the S-tether (3) works well for most cases where the buoyancy of each cable float is greater than 862 N (40.0 lb). If a longer buoyant section (longer than the baseline 700 m) is used, the top and the bottom of the S-tether will shift upward, thus, reducing the maximum allowable buoyancy for the required clearance d_1. If a shorter buoyant section is used, the top and the bottom of the S-tether will shift downward, thus, increasing the minimum allowable buoyancy for the required clearance d_2.

Last, Fig. 9 shows the depth range of the S-tether when the total length of the S-tether is varied from 800 to 2000 m. Extrapolating the figure linearly, it is found that the S-tether must be shorter than 2100 m so that it does not come out of the water, which agrees with (5). If the top of the S-tether is required to be at least 100 m below the water surface and the bottom of the S-tether to be 100 m above the SSF, then the S-tether must be shorter than 1660 m (about 2.4 times the SSF depth). Equation (3), which gives the distance between the top and the bottom of the S-tether, works well in this case.

2) Cable Float Sizes: In the previous section, the minimum requirements for the buoyancy of the cable floats, length of the buoyant section, and the total length of the S-tether were obtained using the configurations under static loading. In this and subsequent sections, the maximum total tensions at the snubber and the anchor, the dynamic motion of the mooring, and the contact stress-slip parameter under dynamic loading are used to find optimal configurations.

First, the effect of differently sized cable floats at different intervals is examined while keeping the total buoyancy of the cable floats at 9792 N (2196 lb) and the length of the buoyant

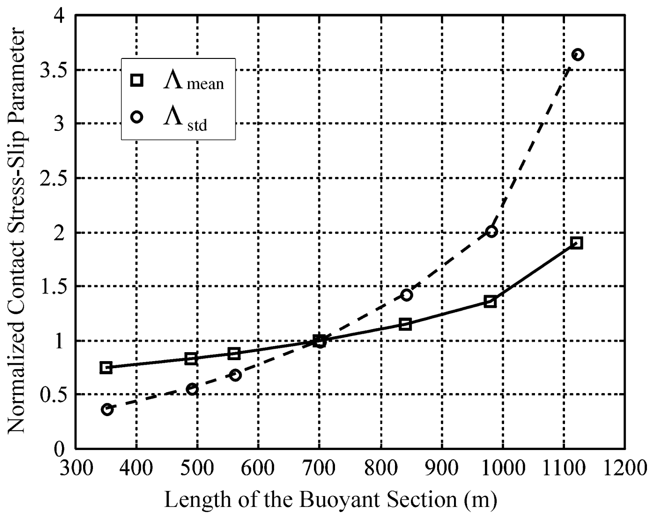

Fig. 10. Effect of varying buoyant section length on the contact stress-slip parameter.

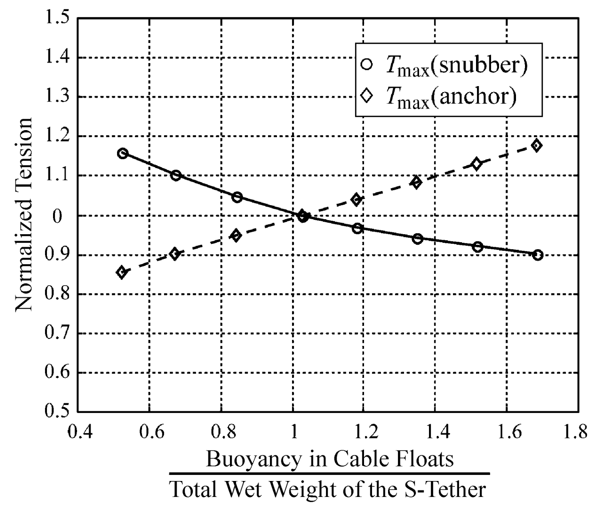

Fig. 11. Effect of varying cable float buoyancy on the maximum tensions.

section at 700 m. For example, twenty-six 376.2-N (84.46 lb) cable floats placed every 28 m provide 9792 N of buoyancy over 700 m.

If N denotes the total number of cable floats, then the buoyancy of each float is proportional to N^{-1}, the diameter of cable floats is proportional to the cube root of the buoyancy or $N^{-1/3}$, and the drag of each cable float is proportional to the diameter squared or $N^{-2/3}$. The total drag is then proportional to $N^{1/3}$. Therefore, the total drag increases with increasing the number of cable floats. When 11 (70 m apart) to 71 cable floats (10 m apart) are used, the drag on the cable floats increases by a factor of 1.86, but the maximum tensions varied by less than 3% (results not shown). Therefore, it is found that the size of the cable floats has little impact on the overall response as long as the total buoyancy and the length of the buoyant section are kept constant.

3) Buoyant Section Length: The length of the buoyant section is varied while keeping the buoyancy of the cable floats at 9792 N (2196 lb) and the total length of the S-tether at 1400 m. Although it was found in the previous section that the size of the cable floats has a minimal effect on the overall dynamics, care is taken so that the same number of same-size cable floats is used (thirty-six 272-N cable floats) for all cases. For example, if the buoyant section is 350 m, the cable floats are placed at 10-m intervals, and the weighted section is 1150 m. If the length of the buoyant section is 980 m, the cable floats are placed at 28-m intervals, and the weighted section is 420 m.

As the buoyant section becomes longer, the maximum tensions in the snubber and the anchor are reduced (results not shown), while the contact stress-slip parameter above the SSF increases (Fig. 10). However, for the range of lengths of the buoyant section used in the analysis (from 350 to 1150 m out of possible 1400 m), the maximum tensions vary by less than $\pm 10\%$ (results not shown). Conversely, Λ_{std} varies from -60% to 365% from that of the baseline design with a significant increase occurs for S-tether lengths greater than 1000 m. Recall that the length of the buoyant section is limited by the configuration of the mooring under the slack condition. It was previously found that the buoyant section must be shorter than 960 m, and if a 100-m clearance between the surface and the top portion of the S-tether is needed, it must be shorter than 810 m ($\approx$60% of the total S-tether length). Keeping the buoyant section at roughly 60% (or less) of the S-tether helps to avoid significant increases in the bending fatigue.

4) Buoyancy in the S-tether: The buoyancy of the cable floats is varied from 134 to 446 N (from 30.0 to 100 lb) while the length of the S-tether is kept constant. Equivalently, the total buoyancy is varied from 4810 to 16 000 N (from 1080 to 3600 lb). Fig. 11 shows that the maximum tension in the snubber decreases monotonically and the maximum tension at the anchor increases monotonically with increasing buoyancy. This makes sense intuitively since the added buoyancy in the S-tether will increase the tension below and decrease the tension above the buoyant section. When 134-N (30.0 lb) cable floats are used, the maximum tension in the snubber increases by 17%, whereas the maximum tension at the anchor decreases by 15%. As the buoyancy increases, the decrease in the maximum snubber tension becomes smaller while the maximum anchor tension continues to increase steadily. Therefore, increasing the buoyancy of the cable floats is effective only to a certain degree.

Fig. 12 shows that the values of Λ_{mean} and Λ_{std} decrease with increasing buoyancy. When the buoyancy of a cable float is 134 N (30.0 lb), the value of Λ_{mean} increases by more than three times, and Λ_{std} by more than five times those of the baseline design. Therefore, if one is concerned with the bending fatigue failure at the connection between the SSF and the cable, the total buoyancy provided by the cable floats should be equal to or greater than the total wet weight of the S-tether.

5) S-Tether Length: The length of the S-tether is varied while the depth of the SSF is kept constant. The total length is varied from 800 to 2000 m. Fig. 13 shows that the maximum tension at the anchor decreases monotonically with increasing S-tether length. The maximum tension in the snubber has a minimum at around 1400 m. Therefore, the S-tether should be at least 1400 m long, which is about twice the SSF depth. The total length of the S-tether is limited by the mooring configuration under slack conditions. Previously, it was found that the S-tether

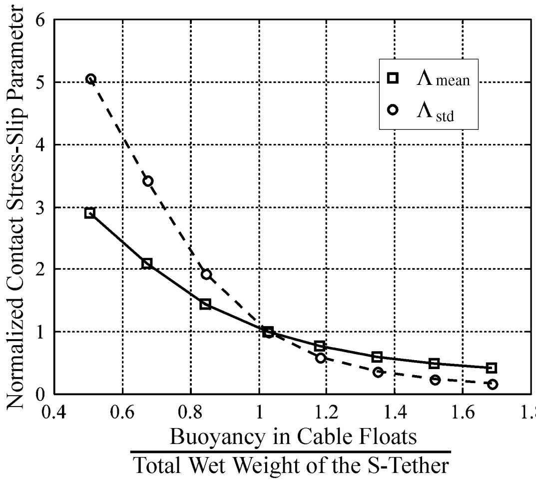

Fig. 12. Effect of varying cable float buoyancy on the contact stress-slip parameter.

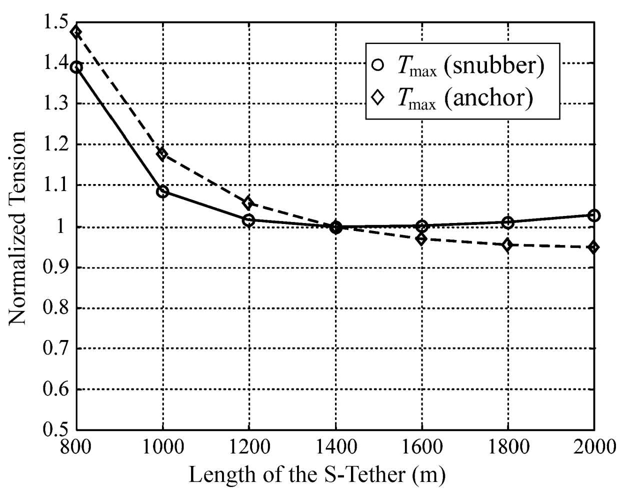

Fig. 13. Effect of varying length of the S-tether on the maximum tensions.

should be shorter than 1660 m for a 100-m clearance above the SSF and below the water surface and must be shorter than 2100 m so that no parts of the mooring line come out of the water under slack conditions.

When the S-tether length is shorter than 1200 m (800 and 1000 m in Fig. 13), an interesting phenomenon occurs. The maximum dynamic tension occurs at the anchor instead of in the snubber. This is because T_{std} at the anchor increases with decreasing S-tether length while the value at the snubber stays about the same (Fig. 14). When the maximum dynamic tension occurs at the anchor, the overall maximum tension in the mooring cable is large especially below the SSF.

Fig. 15 shows that Λ_{mean} peaks for an S-tether length of 1000 m. Similarly, Λ_{std} peaks for an S-tether length of 900 m, though the variation in Λ_{std} is larger. The cable makes a smoother S-shape with increasing S-tether length, and it makes a taut mooring with decreasing S-tether length. Therefore, it makes sense intuitively that the worst case occurs when the S-tether is not long enough to make a smooth curve but not short enough to make a taut line. Of these two options, a short S-tether must be avoided since the tension along the cable may

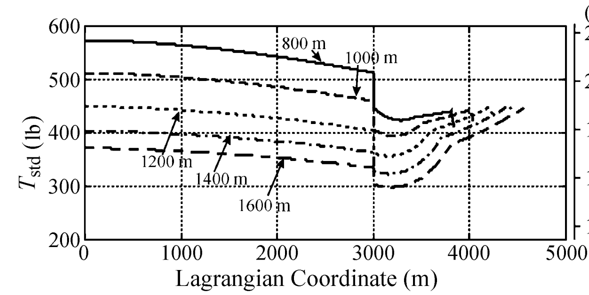

Fig. 14. Standard deviation of the tension for different S-tether length.

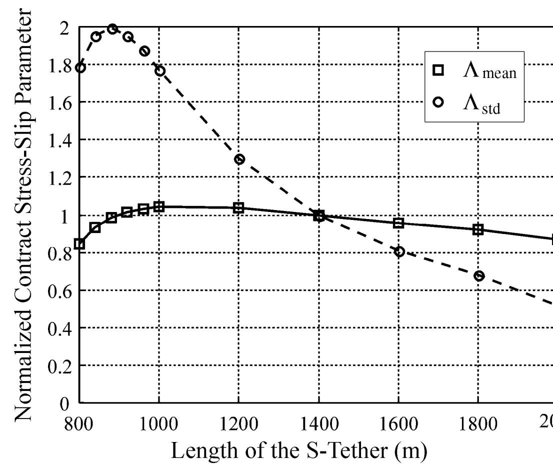

Fig. 15. Effect of varying length of the S-tether on the contact stress-slip parameter.

be too high. Since the maximum tension generally decreases with increasing length, the S-tether should be made as long as possible with the limitation on the length dictated by the mooring configuration under slack conditions.

6) S-Tether Length for Other SSF Depths: Previously, it was found that the optimum S-tether length is about 1400 m when the SSF depth is 700 m. This is twice the SSF depth. In this section, it will be established whether this relationship holds for other SSF depths. Fig. 16 shows the maximum tension in the snubber and the anchor as a function of the S-tether length for various SSF depths between 100 and 700 m. Again, the maximum tension at the anchor decreases with increasing S-tether length, but the maximum tension in the snubber has minimum values. Overall, the mooring performs better when the SSF is placed at a shallower depth. For SSF depths between 100 and 1000 m, the optimal S-tether length for which the maximum snubber tension under the survival condition is a minimum roughly follows the relationship

$$L_{\text{optimum}} \approx 700 + d. \tag{6}$$

One should be careful when placing the SSF at shallow depths. Previously, it was discussed that the length should not be greater than three times the depth of the SSF so that the mooring does not come out of the water under slack conditions. An SSF depth of less than 350 m results in the use of an S-tether shorter than the optimum. Fortunately, the mooring still performs well for S-tether lengths slightly shorter than

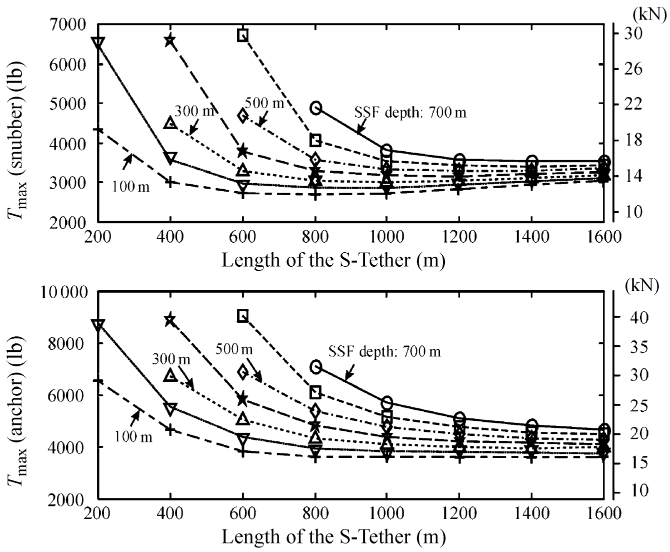

Fig. 16. Effect of varying the SSF depth.

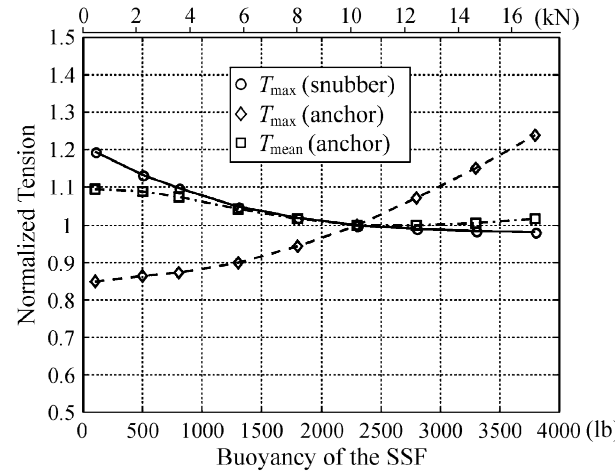

Fig. 17. Effect of varying SSF buoyancy on the maximum tensions.

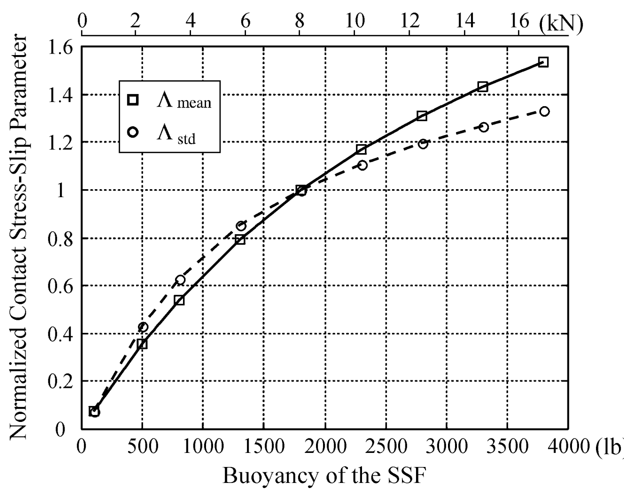

Fig. 18. Effect of varying SSF buoyancy on the contact stress-slip parameter.

the optimum. For instance, if the SSF depth is 300 m, the optimal S-tether length is about 1000 m [based on (6)], but the S-tether should be shorter than three times the SSF depth (5) or 900 m so that no part of the S-tether comes out of the water under slack conditions. Fig. 16 shows that when the S-tether is 600-m-long, the mooring performs better (in terms of the maximum tensions) than the baseline design. When the SSF depth becomes shallower, this is no longer true. For instance, for an SSF depth of 100 m, the optimal S-tether length is about 800 m under survival conditions, while the maximum allowable S-tether length is about 300 m. When the S-tether is 300 m, the mooring performs slightly worse than the baseline design. If a 200-m S-tether is used to have a combined clearance of 50 m, the maximum tensions are about 25%–35% larger than those of the baseline design.

In summary, under the survival condition, a mooring system with an SSF placed at a shallower depth can perform better under the survival condition if the length of the S-tether is chosen appropriately. However, if the SSF is placed too shallow (shallower than 350 m), one is forced to use an S-tether shorter than the optimum so that part of the mooring does not come out of the water during slack conditions.

7) Buoyancy of Subsurface Float: The buoyancy of the SSF is varied from 0 to 17 000 N (3800 lb). Fig. 17 shows that the maximum tension in the snubber decreases and the maximum tension at the anchor increases as the SSF buoyancy increases. This is similar to the previous case of varying buoyancy of the cable floats, which are attached to the S-tether just above the SSF. When the buoyancy of the SSF is zero (i.e., no SSF), the maximum tension at the anchor decreases by 13% while the maximum tension in the snubber increases by 20% from the values of the baseline design. When the buoyancy is increased to 16 900 N (3800 lb), the maximum tension at the anchor increases by 25% while the maximum tension in the snubber and the value of $T_{\rm std}$ at the anchor stay about the same. Note that there is little variation in the maximum tension of the snubber for buoyancy greater than 10 200 N (2300 lb). Similarly, the decrease in the maximum tension at the anchor becomes smaller for buoyancy values smaller than 5791 N (1300 lb). Therefore, the optimal buoyancy lies between 5800 and 10 200 N. For a reference, these values are much larger than the total weight of the cable that hangs below the SSF [total cable weight in water is approximately 1500 N (337lb)]. When a similar mooring is placed in a 1800-m-deep water (with SSF depth of 300 m and an S-tether length of 600 m), the optimum value is also between 5800 N and 10 200 N. Therefore, the required buoyancy depends strongly on the environmental input and weakly on the weight of the mooring line hanging below the SSF.

Fig. 18 shows that both $\Lambda_{\rm mean}$ and $\Lambda_{\rm std}$ increase with increasing buoyancy. This is opposite from what was seen when the cable float buoyancy was increased. In that case, both $\Lambda_{\rm mean}$ and $\Lambda_{\rm std}$ decreased. This makes sense intuitively since smaller SSF buoyancy may provide smoother transition between the lower and the upper cable.

Fig. 19 shows the horizontal offset under the survival conditions when the buoyancy of the SSF is varied. When the buoyancy is decreased to 445 N (100 lb), the static configuration is close to that of a line.

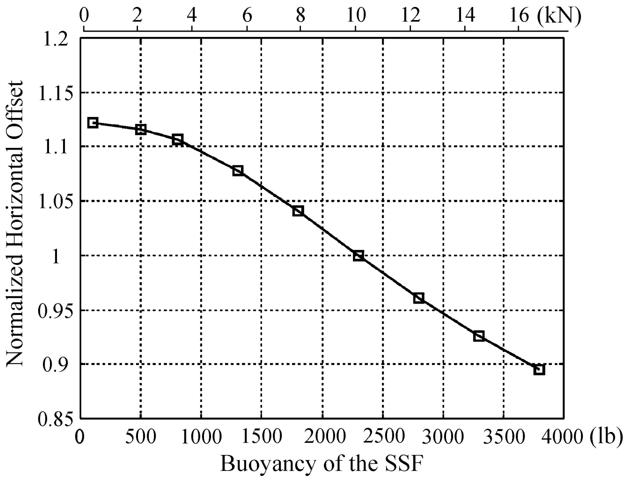

Fig. 19. Static horizontal offset of the surface buoy under the survival condition for various SSF buoyancy.

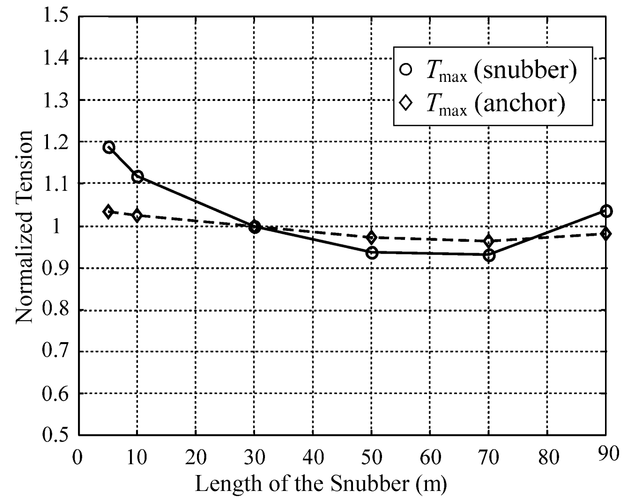

Fig. 21. Effect of varying snubber length on the maximum tensions.

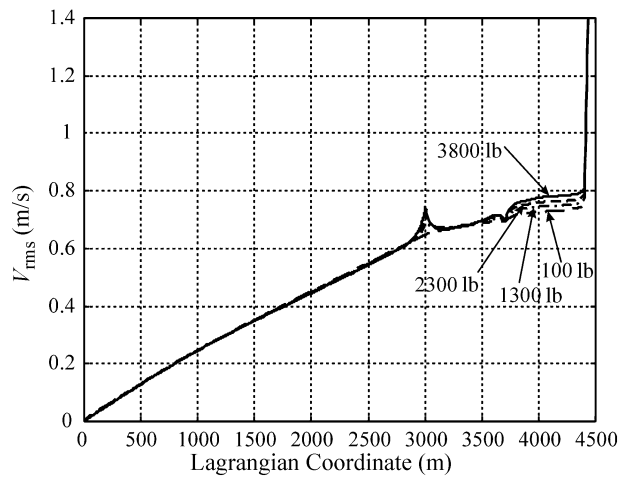

Fig. 20. RMS speeds along the cable for various SSF buoyancy.

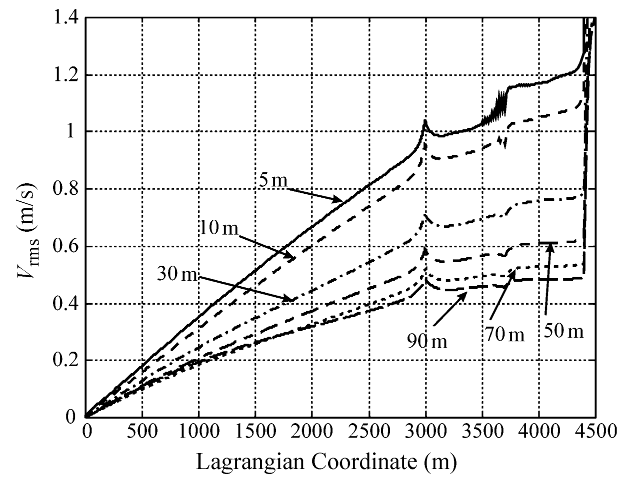

Fig. 22. RMS speeds for various snubber hose lengths.

Fig. 20 shows the rms speed along the cable for four SSF with different buoyancy. It shows that the speeds are comparable and the size of the SSF has little effect on the speed of the cable.

8) Snubber Hose Length: The length of the snubber hose is varied from 5 to 90 m. Although it is not shown here, it is found that increasing snubber length generally increases overall mean tension while decreasing the overall dynamics below the snubber hose. If the increase in T_{mean} is greater than four times the decrease in T_{std}, then the maximum tension increases. This happens when the snubber length is about 70 m, where the maximum tensions start to increase. Fig. 21 shows that the optimal snubber length is 70 m, where both quantities are at the minimum. It should be noted that nearly as good results with a 30-m snubber could be obtained. Therefore, if it is not critical to lower the tension in the snubber, a 30-m snubber may be sufficient.

Fig. 22 shows that most of the dynamics (in terms of the standard deviation of speed) is reduced dramatically over the length of the snubber. Therefore, it is important to have a sufficiently long snubber if the motion of the cable needs to be small (e.g., for subsea activities).

9) Summary for Mooring With a Subsurface Float: The most important parameter affecting the maximum tensions in the snubber and at the anchor is the length of the S-tether. The optimal S-tether length under survival conditions depends on the depth of the subsurface buoy. If the subsurface buoy is placed too shallow, the optimal length may be too long under the slack condition, therefore, forcing the designer to use a shorter-than-optimal length. The most important parameter affecting the speed of the cable is the snubber length. Most of the dynamic motion (in terms of rms speed) is reduced over the length of the snubber hose that makes up part of the S-tether. The most important parameter affecting the bending fatigue is the buoyancy and the length of the buoyant section. The buoyancy must be such that the cable floats support at least the wet weight of the S-tether, and the length should not be greater than 60% of the total length of the S-tether.

B. Mooring Without a Subsurface Float

The configuration of the mooring design without an SSF is given in the Appendix. The baseline design consists of a surface buoy, a 30-m snubber hose, an 800-m armor-jacketed Vectran EOM cable, a 1925-m Vectran EOM cable, a 420-m cable with twenty-two 136-N (30.5 lb) cable floats at 20-m intervals (lower buoyant section), a 1440-m Vectran cable, a 5-m potted

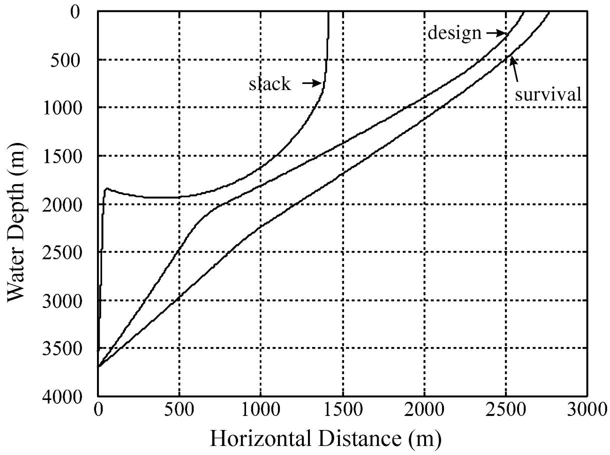

Fig. 23. Static configurations of the mooring without a SSF under the slack, design, and survival currents.

chain, and an anchor placed in a 3700-m-deep water. The baseline design has a scope of 1.25. In this section, the buoyancy of the cable floats, length of the buoyant sections, total length of the mooring, and snubber length will be varied.

Fig. 23 shows the static configurations due to wind and current. The horizontal offset of the surface buoy extends to 2660 m in design conditions and 2750 m in the survival condition. Both of these values are close to the maximum horizontal offset of 2775 m predicted by (2). This shows that it is difficult to limit the horizontal offset of the mooring without an SSF in moderate to high currents. The resulting configuration of nearly a straight line no longer provides geometric compliancy.

Fig. 24(a) and (b) shows the mean and the standard deviation of the tension under the survival and design conditions. Note that both $T_{\rm mean}$ and $T_{\rm std}$ under the design condition are significantly less than those under the survival condition, and even more so than the previous design with an SSF. For example, the maximum snubber tension is reduced by a factor of 2.5, and the maximum anchor tension by a factor of 2.2, whereas the numbers are 2.0 and 1.6, respectively, for the mooring with an SSF (Fig. 4; Table I). If the maximum tensions under the survival condition are comparable in the two designs, it can be expected that the design without an SSF will be subjected to smaller loads than the design with an SSF under less severe conditions.

Under both design and survival conditions, the mean tension along the cable does not vary significantly, but the dynamic tension increases along the cable from the snubber hose to the anchor. Therefore, the maximum tensions at the anchor (Table II) are slightly larger than those in the snubber.

Fig. 24(c) shows the rms speed along the cable. The rms speeds are reduced dramatically over the snubber, and they are somewhat lower right below the snubber hose than those of the design with an SSF [Fig. 4(c)]. Note that the rms speed in the lower buoyant section under the design and survival conditions are comparable.

Fig. 25 shows the mean and the standard deviation of the contact stress-slip parameter. Both values are large where the cable floats are attached in the lower section and highest where the lower buoyant section ends. In this paper, $\Lambda_{\rm mean}$ and $\Lambda_{\rm std}$ will be monitored at this location. Note that the maximum $\Lambda_{\rm mean}$ and

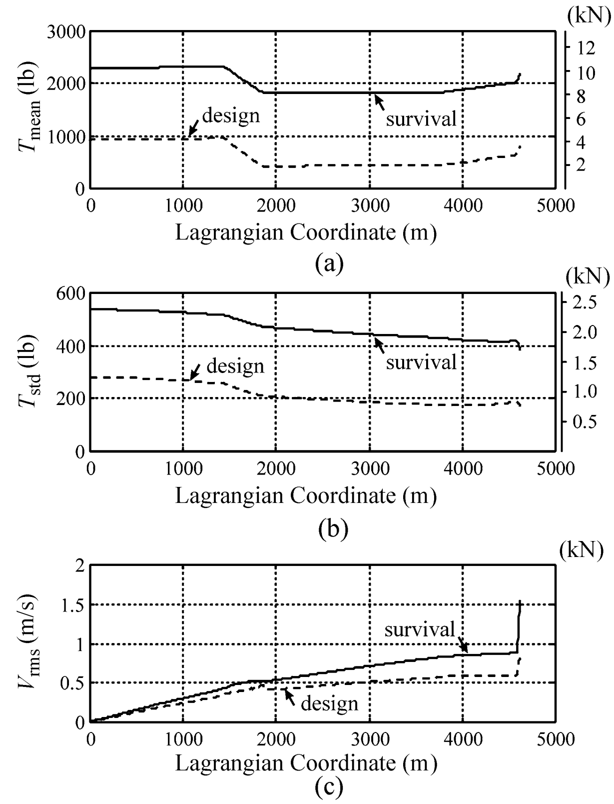

Fig. 24. Mean tension, standard deviation of the tension, and standard deviation of the speed under the survival and design conditions.

TABLE II
MAXIMUM TENSIONS OF THE BASELINE DESIGN

$T_{\rm max} = T_{\rm mean} + 4T_{\rm std}$	Snubber (N)	Anchor (N)
Design condition	6680	8950
Survival condition	16600	19600

$\Lambda_{\rm std}$ of the design without an SSF (at the end of lower buoyant section) are lower than those with an SSF (just above the SSF).

1) Total Length: The total length of the mooring is varied from 3752 to 5935 m (scope from 1.01 to 1.60) by varying the length of each component (with the exception of 5-m chains and snubber) from 81% to 128% of its original value. The buoyancy per unit length in the lower buoyant section is kept constant (not shown). For instance, a 3752-m mooring consists of a surface buoy, a 30-m snubber hose, a 648-m armor-jacketed Vectran EOM cable, a 1558-m Vectran EOM cable, a 340-m Vectran EOM cable with eighteen 136-N (30.5 lb) cable floats, a 1166-m Vectran EOM cable, a 5-m chain, and an anchor.

Fig. 26 shows that increasing the scope of the mooring improves performance. By increasing the scope from 1.25 to 1.60, the maximum tensions at the anchor and in the snubber decrease by 18% and 19%, respectively. The contact stress-slip parameter, on the other hand, does not vary much with the length mooring (not shown here).

2) Buoyant Section: In this section, some issues concerning the buoyant section such as the location, length, buoyancy, and size of the cable floats will be discussed. The buoyancy of the buoyant section of the baseline design is 2990 N (671 lb). This

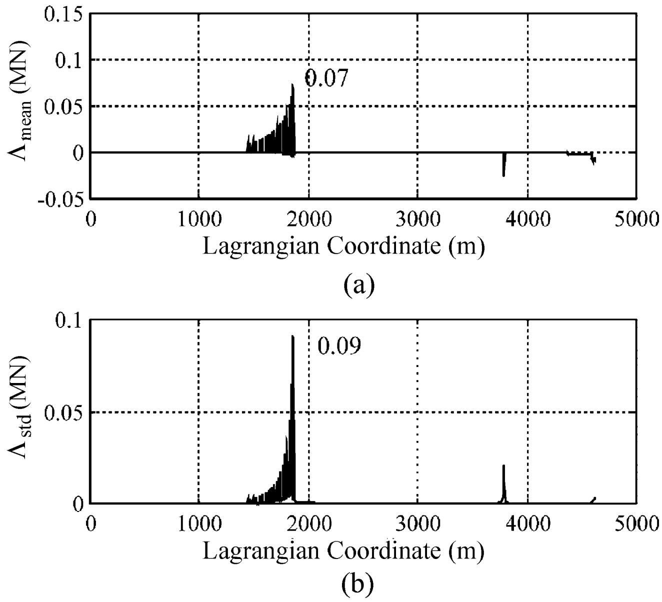

Fig. 25. Mean and the standard deviation of the contact stress-slip parameter.

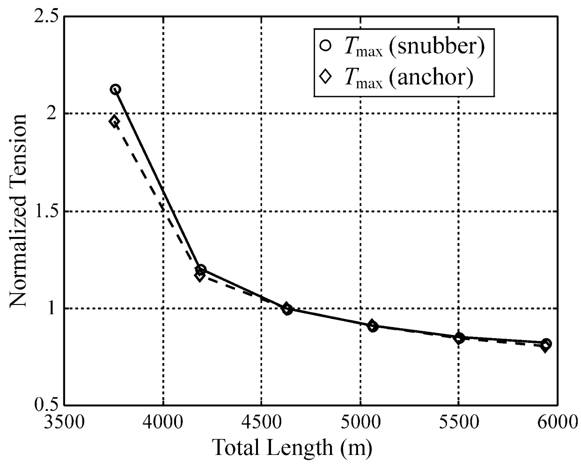

Fig. 26. Effect of varying total length.

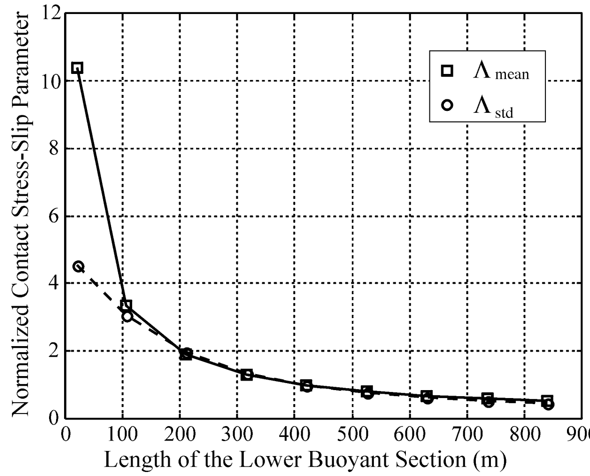

Fig. 27. Effect of varying length of the lower buoyant section on the contact stress-slip parameter.

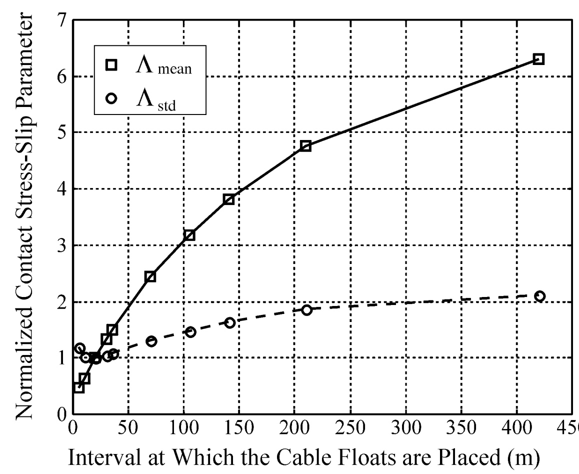

Fig. 28. Effect of distribution of cable floats on the contact stress-slip parameter.

compares to the maximum total anchor tension in survival conditions of 19 600 N (4410 lb). It is known from previous experience that an increase in the buoyancy of any of the mooring components generally increases the tension at the anchor. In this case, since the buoyancy provided by the cable floats is a small fraction of the maximum total anchor tension, it would take a large increase in the buoyancy of the buoyant section to significantly affect the variations in the maximum total tension at the anchor. It was found that if the buoyancy is doubled from its baseline value (either by doubling the buoyancy of each of baseline cable floats, halving the spacing between cable floats, or doubling the length of the buoyant section while maintaining the baseline spacing of cable floats), the maximum total tension at the anchor increases by less than 10% and the maximum total tension in the snubber increases by less than 2%. Therefore, it is concluded that the buoyancy, length, and how the cable floats are distributed over the buoyant section (for a range of realistic values) do not affect the maximum total tensions of the mooring significantly. It was also found that the location of the buoyant section had little effect on the maximum total tensions.

The story is different for the contact stress parameter. Fig. 27 shows Λ_{mean} and Λ_{std} when the length of the buoyant section is varied from 21 to 840 m with 136-N (30.5 lb) cable floats spaced every 20 m as in the baseline case. Both quantities improve significantly with increasing length of the buoyant section. Next, the size of the cable floats is varied while keeping the length and the total buoyancy of the buoyant section constant at 420 m. For example, starting with eighty-five 35.1-N (7.89 lb) cable floats placed at 5-m intervals, it went down to two 1500-N (336 lb) cable floats at a 420-m interval. Fig. 28 shows the variation in the contact stress-slip parameter with the differently sized cable floats and different interval lengths. As larger and more coarsely spaced cable floats are used, both Λ_{mean} and Λ_{std} increase. Therefore, it is better to use smaller cable floats distributed over a longer distance or, in the best case scenario, to use a continuous buoyant jacket.

3) Snubber Hose Length: Fig. 29 shows the rms speed along the cable when the snubber hose length is varied from 10 to 90 m. The dynamic motion below the snubber hose decreases

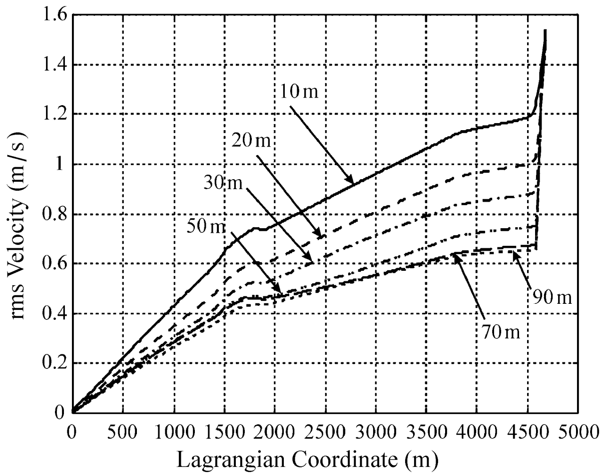

Fig. 29. RMS speed along the cable under the design condition.

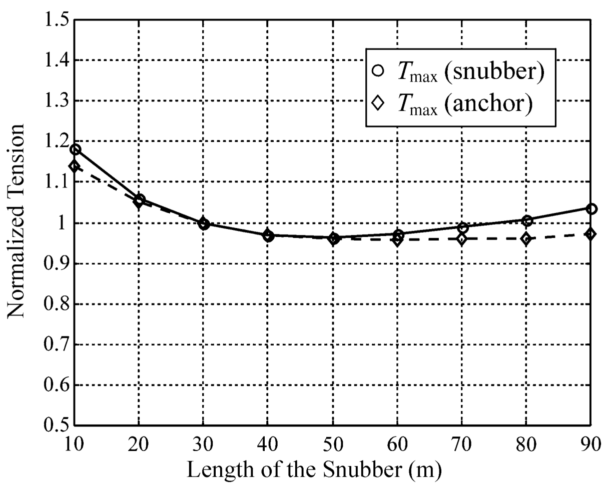

Fig. 30. Effect of varying snubber length on the maximum tensions.

rapidly with increasing snubber hose length up to 70 m. The maximum total tensions (Fig. 30) reach their minima when snubber length is between 50–70 m, but the snubber length of 30 m still gives relatively good results. It is not advisable to use a snubber shorter than 30 m since the maximum tensions and the dynamic motion increase rapidly for a snubber length shorter than 30 m. The contact stress-slip parameter along the mooring line (not shown) does not vary much with the snubber length.

4) Summary for the Mooring Without a Subsurface Float: The most important parameter affecting the maximum tensions in the snubber and at the anchor is the length of the mooring. The most important parameter affecting the dynamic motion of the cable is the snubber length since most of the dynamics (measured by rms speed) is reduced over the length of the snubber hose. The most important parameters affecting the bending fatigue in the buoyant section are the length of the buoyant section and the distribution of the cable floats. A longer buoyant section gives better results. For a given buoyant section length, smaller and more closely packed floats (or continuous flotation) give the best results.

TABLE III
COMPARISON OF THE TWO TYPES OF MOORING SYSTEM AT 3700-m WATER DEPTH

Scope	$T_{\max}$ (snubber) (N)	$T_{\max}$ (anchor) (N)	$x_{\rm SB}$ (m)
With, 1.20	16 800	23 000	2200
Without, 1.03	35 300	38 400	830
1.20	17 900	21 000	2400
1.25	16 600	19 600	2770
1.37	15 100	16 600	3390
1.60	13 700	15 800	4550

TABLE IV
COMPARISON OF THE TWO TYPES OF MOORING SYSTEM AT 1800-m WATER DEPTH

Scope	$T_{\max}$ (snubber) (N)	$T_{\max}$ (anchor) (N)	$x_{\rm SB}$ (m)
With, 1.17	14 600	20 300	1090
Without, 1.16	21 000	22 900	1070
1.28	18 000	20 100	1430
1.53	15 000	17 100	2080
1.78	13 500	15 700	2640

C. Comparison Between the Moorings With and Without a Subsurface Float

The baseline design with an SSF is compared to designs of varying scope without an SSF. Table III lists the maximum tensions and the horizontal offsets of the surface buoy under the survival condition. For the same scope, the maximum snubber tension, the maximum anchor tension, and the horizontal offset of the surface buoy are comparable. However, as the scope increases in the design without an SSF, the tensions can be lowered significantly at the cost of large offset, whereas the design with an SSF with a scope of 1.2 is already optimized for maximum tensions. Recall that if the maximum tensions are comparable in two designs under survival conditions, then the design without an SSF is subjected to smaller loads under less severe condition.

It is also found that the design without an SSF is much better in terms of the bending fatigue damage based on the moorings considered here (Figs. 5 and 25). The calculated bending fatigue damage can be improved in the design with an SSF if the moment is properly released. However, the operational history of moorings with SSFs has shown that bending fatigue damage is a common failure modes, and therefore, the design without an SSF should be used if the bending fatigue may be an issue.

The same analysis is performed for the mooring in 1800 m, and the results are shown in Table IV. For the same scope, the maximum tensions in the design with an SSF are significantly lower than those in the design without an SSF. However, the maximum tensions in the design without an SSF can, again, be lowered significantly with increasing scope.

The design without an SSF provides a long smooth section of cable without the interruptions of cable floats or subsurface buoys. This is a clear design advantage if the mooring is to be used with a near-surface profiler that moves up and down the cable in the upper water column.

In summary, the design with an SSF can be optimized for maximum tensions by choosing an appropriate S-tether length. In this case, the maximum snubber tension and the horizontal offset are smaller than those of the design without an SSF with

TABLE V
PROPERTIES OF THE VECTRAN CABLE AND SNUBBER

	Vectran, Steel-Armored, Armor-Covered Cable
EA (MN)	5, 10, 10
EI (N•m^2)	0.1, 0.5, 0.5
GJ (N•m^2)	0.5, 1, 1
Mass/length (kg/m)	0.477, 0.877, 1.042
Added mass/length (kg/m)	0.426, 0.520, 0.240
Diameter (m)	0.0230, 0.0254, 0.0285
C_{dt}	0.0, 0.0, 0.0
C_{dn}	1.5, 1.5, 1.5
Wet weight (N)	0.1, 6.8, 1.345

TABLE VI
PROPERTIES OF THE CABLE FLOATS

	SSF	272 N Cable Float
Diameter (m)	1.54	0.5657
Mass (kg)	921	35.7
Added mass (kg)	1909	28.6
Wet weight (N)	−10 235	−272
C_{dt}	0.2	0.2
C_{dn}	0.8	1

TABLE VII
PROPERTIES OF THE VECTRAN STRAND

Layer	Number of Wires	E (MPa)	Wire Diameter (mm)	Lay Angle (°)
1	30	200	3.54	17.74
2	24	117	3.54	-16.45
3	18	117	3.54	-15.93
4	12	117	3.54	14.90
5	7	117	3.54	15.52
King	1	117	5.05	

the same scope under survival conditions. However, the maximum tensions in the design without an SSF can be lowered by increasing the scope of the mooring. The design without an SSF is also subject to smaller bending fatigue and has an advantage when a near-surface profiler is required.

IV. Conclusion

For the design with a SSF, the most important design parameter in terms of the maximum tensions is the length of the S-tether. The optimal length of the S-tether under survival conditions depends on the depth of the subsurface buoy. If the subsurface buoy is placed too shallow, the optimal length may be impractical under the slack condition. Steel-armored cable is susceptible to bending fatigue damage just above the SSF if the moment is not released properly at that location. The contact stress-slip parameter is most sensitive to changes in the length and the buoyancy of the buoyant section of the S-tether. The length of the buoyant section should be around 60% of the total S-tether length, and the total buoyancy provided by the cable floats should be at least equal to the total wet weight of the S-tether. The dynamic motion in the cable is governed by the length of the snubber hose. The snubber hose must be at least 30 m long to keep the dynamic motion reasonably small.

For the design without an SSF, the maximum tensions can be lowered significantly by increasing the scope. In fact, the tensions can be made much lower than the optimum values in the design with an SSF. The cable is most susceptible to bending fatigue where cable floats are attached. The contact stress-slip parameter is most sensitive to the size and the distribution of the cable floats. It is better to distribute the cable floats over a longer length. For a given distance, it is better to use smaller and more closely packed cable floats or better yet a continuous buoyant jacket. When compared to the design with an SSF, the contact stress-slip parameter is much smaller in the design without an SSF. The total buoyancy and the location of the buoyant section, however, do not significantly affect the maximum tensions and the bending fatigue. The location and magnitude of the buoyancy must be such that no part of the cable touches the ocean floor under slack conditions. Again, the dynamic motion in the cable is governed by the length of the snubber hose, and the length must be at least 30 m.

The design with an SSF should be used if a small watch circle and small tension in the snubber are required. The design without an SSF is preferred if small overall tension is required even at the cost of large offset, if bending fatigue failure is of concern, and if the use of a profiler is required.

Appendix

Configuration for the mooring system with an SSF is as follows:

1) anchor;
2) 5-m potted chain;
3) 2990-m Vectran cable;
4) 5-m potted chain;
5) 10 200-N (2300 lb) SSF;
6) 5-m potted chain;
7) 700-m steel-armored cable with thirty-six 272-N (61 lb) cable floats at 20-m intervals;
8) 700-m steel-armored cable;
9) 13.35-kg coupling;
10) 30-m snubber.

Configuration for the mooring system without an SSF is as follows:

1) anchor;
2) 5-m potted chain;
3) 1440-m Vectran cable;
4) 420-m Vectran cable with twenty-two 136-N (30.5 lb) cable floats at 20-m intervals;
5) 1925-m Vectran cable;
6) 5-m potted chain;
7) 800-m armor-covered Vectran cable;
8) 13.35-kg coupling;
9) 30-m snubber.

The properties of the cables and floats used are given in Tables V and VI. The surface buoy is modeled as a cylinder. The mass is 3200 kg, the diameter is 3.2 m, the height is 1.5 m, the surface area exposed in the air is 6.2 m^2, the wind drag coefficient is 1.5, and the normal fluid drag coefficients is 1.

References

[1] R. Detrick, D. Frye, J. Collins, J. Gobat, M. Grosenbaugh, R. Petit, A. Plueddeman, K. Von der Heydt, B. Wooding, J. Orcutt, J. Berger, R. Harriss, F. Vernon, J. Halkyard, and E. Horton, *DEOS Moored Buoy Observatory Design Study*. Arlington, VA: National Science Foundation/Ocean Science Division, 2000.

[2] National Research Council of the National Academy of Science, *Illuminating the Hidden Planet: The Future of Seafloor Observatory Science*. Washington, DC: The National Academies Press, 2000.

[3] M. Chaffey, E. Mellinger, and W. Paul, "Communications and power to the seafloor: MBARI's ocean observing system mooring concept," in *Proc. OCEANS*, Honolulu, HI, 2001, pp. 2473–2481.
[4] Ocean Studies Board, *Enabling Ocean Research in the 21st Century: Implementation of a Network of Ocean Observatories*. Washington, DC: The National Academies Press, 2003.
[5] W. Paul and D. Bently, "Conductor survival in lightweight upper ocean working cables," in *Proc. Int. Offshore and Polar Eng. Conf. (ISOPE)*, Stavanger, Norway, 2001, vol. 2, pp. 708–714.
[6] J. H. Evans and J. C. Adamchak, *Ocean Engineering Structures*. Cambridge, MA: MIT Press, 1969.
[7] H. O. Berteaux, *Buoy Engineering*. New York: Wiley, 1976.
[8] R. H. Canada and D. R. May, "Mooring developments and design philosophy at the National Data Buoy Center," in *Proc. OCEANS*, San Diego, CA, 1985, pp. 1336–1343.
[9] Z. L. Machado and J. M. Dumay, "Dynamic production riser on Enchova field offshore Brazil," presented at the Offshore Brazil Conf., Latin America Oil Show, Rio de Janeiro, Brazil, 1980, unpublished.
[10] American Petroleum Institute, "Recommended Practice for Flexible Pipe" Washington, DC, RP 17B, 2002.
[11] F. B. Seyed and M. H. Patel, "Parametric studies of flexible risers," in *Proc. 1st Int. Offshore Polar Eng. Conf.*, Edinburgh, U.K., 1991, vol. 2, pp. 147–156.
[12] M. Raoof and R. Hobbs, "Analysis of layered structural strands," *J. Eng. Mech.*, vol. 114, no. 7, pp. 1166–1182, 1988.
[13] M. Raoof, "Axial fatigue of multilayered strands," *J. Eng. Mech.*, vol. 116, no. 10, pp. 2083–2099, 1990.
[14] ——, "Free-bending fatigue of multilayered strands," *J. Eng. Mech.*, vol. 118, no. 9, pp. 1747–1764, 1992.
[15] ——, "Design of steel cables against free-bending fatigue at terminations," *The Structural Engineer*, vol. 71, no. 10, pp. 171–178, 1993.
[16] J. I. Gobat and M. A. Grosenbaugh, "WHOI Cable v2.0: Time Domain Numerical Simulation of Moored and Towed Oceanographic Systems" Woods Hole Oceanographic Inst., Woods Hole, MA, Tech. Rep. WHOI-2000-08, 2000.
[17] ——, "WHOI Cable: Time domain numerical simulation of moored and towed oceanographic systems," in *Proc. OCEANS*, Nice, France, 1998, vol. 3, pp. 1681–1685.
[18] ——, "Dynamics in the touchdown region of catenary moorings," *Int. J. Offshore Polar Eng.*, vol. 11, no. 4, pp. 273–281, 2001.

Seon M. Han received the B.E. degree from the Cooper Union for the Advancement in Science and Engineering in 1996 and the M.S. and Ph.D. degrees from Rutgers, the State University of New Jersey, New Brunswick, in 1998 and 2001, respectively.

She is currently an Assistant Professor in the Department of Mechanical Engineering at Texas Tech University, Lubbock. Her research interests include vibration and dynamics of offshore and marine structures.

Mark A. Grosenbaugh received the B.S. and M.S. degrees from Stanford University, Stanford, CA, in 1976 and 1983, respectively, and the Ph.D. degree from the University of California, Berkeley, in 1987.

He joined the scientific staff at Woods Hole Oceanographic Institution, Woods Hole, MA, in 1987 and is currently an Associate Scientist in the Department of Applied Ocean Physics and Engineering. His research interests include dynamics of moored and towed oceanographic cable systems.